

Supplementary information to:

Emission of fine and ultrafine nanoparticle aerosols from composites functionalized with Multi-Wall Carbon Nano Tubes (MWCNTs) subjected to sliding wear: the influence of matrix material

F. Husanu¹, J. C. Velez^{1, 2}, J.A. Cornelio, J.F. Santa, A. Toro², M. Castellote¹, R. Nevshupa^{1,*}

¹Spanish National Research Council, Eduardo Torroja Institute of Construction Science (IETCC-CSIC), Madrid, Spain

² National University of Colombia, Medellin, Colombia

Abrasion experiments were conducted on two distinct materials: cement paste and epoxy resin, both containing MWCNT additives. For the cement paste experiments, the abrasive material was an alumina sphere, while for the epoxy resin experiments, a steel disk was used as the abrasive.

1. Maximum “flash” temperature at sliding contact

The maximum “flash” temperature at sliding contact for the cement pastes was evaluated using the method described by Kennedy et al., 1994 [1] as following:

Approximate solution for flash temperature (for elastic Hertzian contact, parabolic heat source):

$$\Delta T_{max} = \frac{1.31R\mu\rho_c v}{[K_1\sqrt{(1.2344+Pe_1)}+K_2\sqrt{1.2344+Pe_2}]}, \quad (S1)$$

where R is the size of the contact zone along the direction of sliding, μ is the friction coefficient, p_c is the mean contact pressure, v is the sliding velocity, K_1 is the thermal conductivity, Pe_1 is the Peclet number for flat sample:

$$Pe_1 = \frac{Rv_1}{2k_1}, \quad (S2)$$

where k_1 is the thermal diffusivity.

Subscripts 1 and 2 refer to the flat sample and the pin, correspondingly.

Identical analytical procedures were employed for the polymer samples. The approximate solution (for a uniform square source) was determined by:

$$\Delta T_{max} = \frac{2lq_0\sigma_p}{\left[K_1\sqrt{\pi(1+Pe_1)}\right]} = \frac{2lq_0(1-\sigma_p)}{\left[K_2\sqrt{\pi(1+Pe_2)}\right]}, \quad (S3)$$

where l is half contact length along the sliding direction, q_0 is average heat flux over the contact area, σ_p is the heat partitioning factor:

$$\sigma_p = \frac{1}{1 + \frac{K_2}{K_1} \sqrt{\frac{1+Pe_2}{1+Pe_1}}} \quad (S4)$$

Table S1. Initial parameters for calculation of flash temperature:

Parameters	Cement paste	Alumina ceramic	Vinyl ester polymer	Steel disc
K_1 (W m ⁻¹ K ⁻¹)	70	32	1.07	53
p_c (Mpa)			0.4	
v (m s ⁻¹)	1		3.34	
k_1 (m ² s ⁻¹)	1.60×10^{-7}	1.2×10^{-5}	2.30×10^{-7}	2.28×10^{-5}
$2R$ (m)	2.4×10^{-4}			
l (m)			0.005	
Friction coefficient	0.5		0.5	

Depending on the normal load and variation of other parameters the resulting “flash” temperature increase is ranged between 5 and 20.5 °C.

Contact “flash” temperature for the resin with a velocity of 3.5 m/s: 18.2 °C

Contact “flash” temperature for the polymer at a velocity of 3.7 m/s: 19.2 °C

Contact “flash” temperature for the polymer at a velocity of 4.0 m/s: 20.5 °C

Contact temperature for the cement paste at a velocity of 1.0 m/s: 5 °C

2. Mean temperature increase due to frictional heat dissipation.

For immobile parts ($Pe=0$), mean temperature increase due to the action of the constant heat source at the contact surface with the density q is found from the following expression:

$$\Delta T_{mean} = P\sqrt{t}, (2)$$

where P is a coefficient depending on the material physical properties and sliding velocity.

The values of parameters used for calculation and the calculation results are shown in Table S2.

Table S2. Parameters used for calculation and the results for mean temperature increase at the sliding contact.

Parameters	Vinyl ester polymer component	Mean temperature increase (°C)
v (m/s)		
v_1	3.5	21
v_2	3.7	22
v_3	4.0	24
t (s)	900	
ρ (kg/m ³)	1400	
C_p (J kg ⁻¹ K)	1200	
K_1 (W m ⁻¹ k ⁻¹)	1.26	

3. Water adsorption on cementitious materials

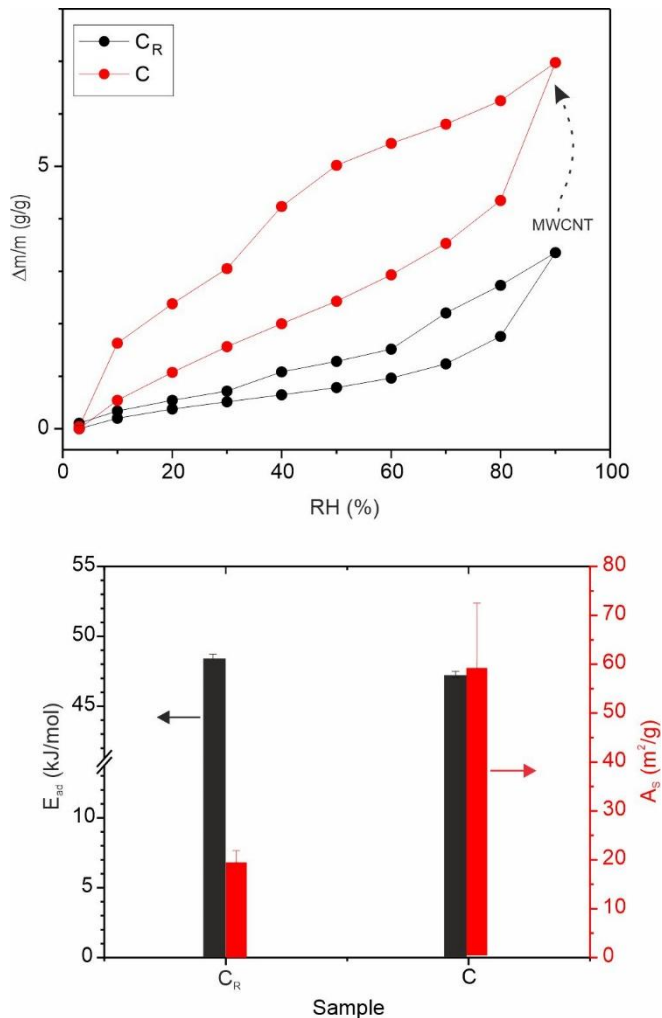


Fig. S1 a) Isotherms of water vapour adsorption on cement paste (Cem_R) and cement-matrix composite (Cem) at 25° C; b) adsorption energy and specific surface area determined from the water vapour adsorption isotherms

The water desorption isotherms of cement paste samples at 25°C show an upward trend with the addition of the additive, as illustrated in Figure 3.2.1 a). These isotherms exhibit typical patterns frequently seen in water adsorption on cement pastes and mortars [2, 3]. These patterns suggest the presence of samples with an open pore structure that include a broad spectrum of pore sizes. Fig. 3.3.1 b) displays the activation energy for desorption and the specific surface area that was estimated using the Brunauer, Emmett, and Teller (BET) method [4]. To ensure accurate BET analysis, the guidelines proposed by Rouquerol et al. were followed [5], using a relative pressure

range of 0.2 to 0.7. Although the BET model may not be ideal for describing water desorption from cement mortars [6], we used it in this study for its simplicity and to facilitate comparisons between different compositions. The results from the BET model fitting are provided in Table S3. While the CNT addition increased the specific surface area, it had no impact on the activation energy for water desorption, as determined from the BET C constant. This suggests a change in pore structure, with more nanopores likely present in the CNT-containing sample [7].

Table S3. BET model fitting results for H₂O adsorption isotherms (mean ± standard errors)

Sample	Intercept (mg/cm ³)	Slope (g/cm ³)	V _m (10 ⁻³ liquid H ₂ O cm ³ /g)	C _{BET}
Cem _R	36.85 ± 5.11	175.76 ± 15.41	4.7 ± 0.77	5.76 ± 0.94
Cem	18.02 ± 3.12	52.62 ± 7.36	14.1 ± 3.1	3.91 ± 0.87

4. Raman spectra

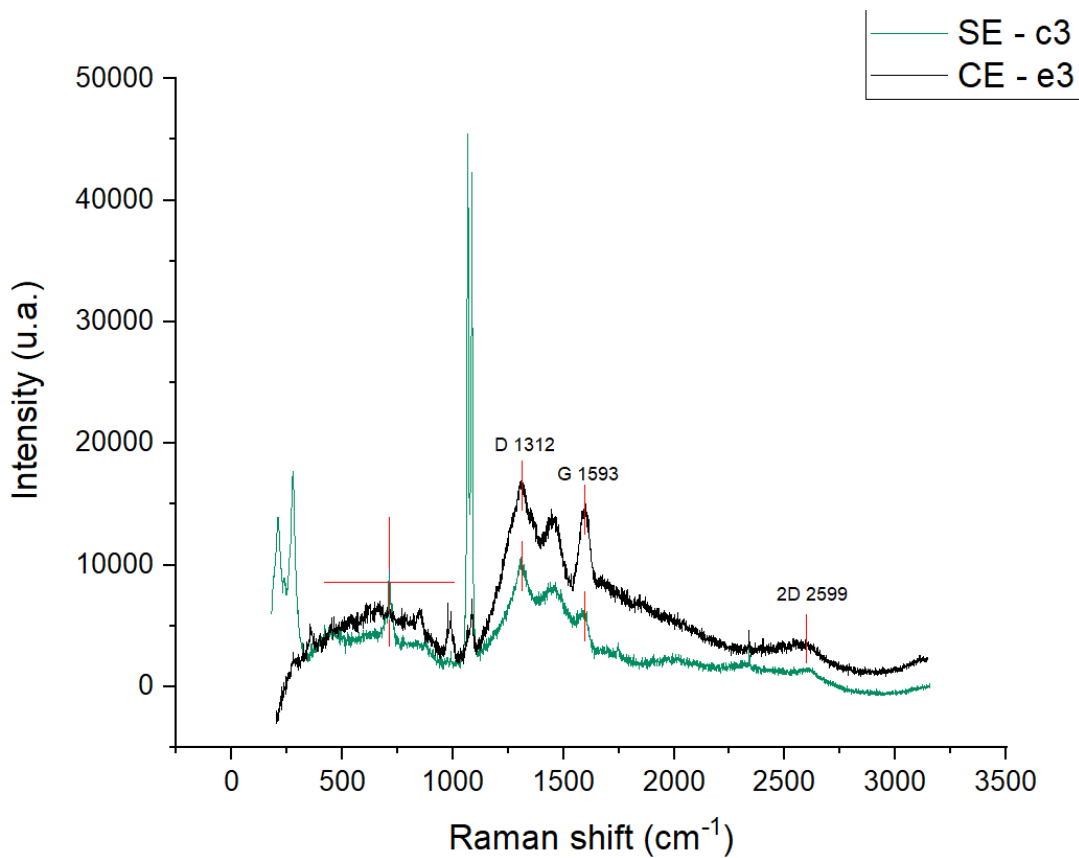


Fig. S2. Raman spectra of pristine (green line) and worn (black line) surfaces of polymer composite.

5. Schematic diagram showing various aspects of aerosol emission studies

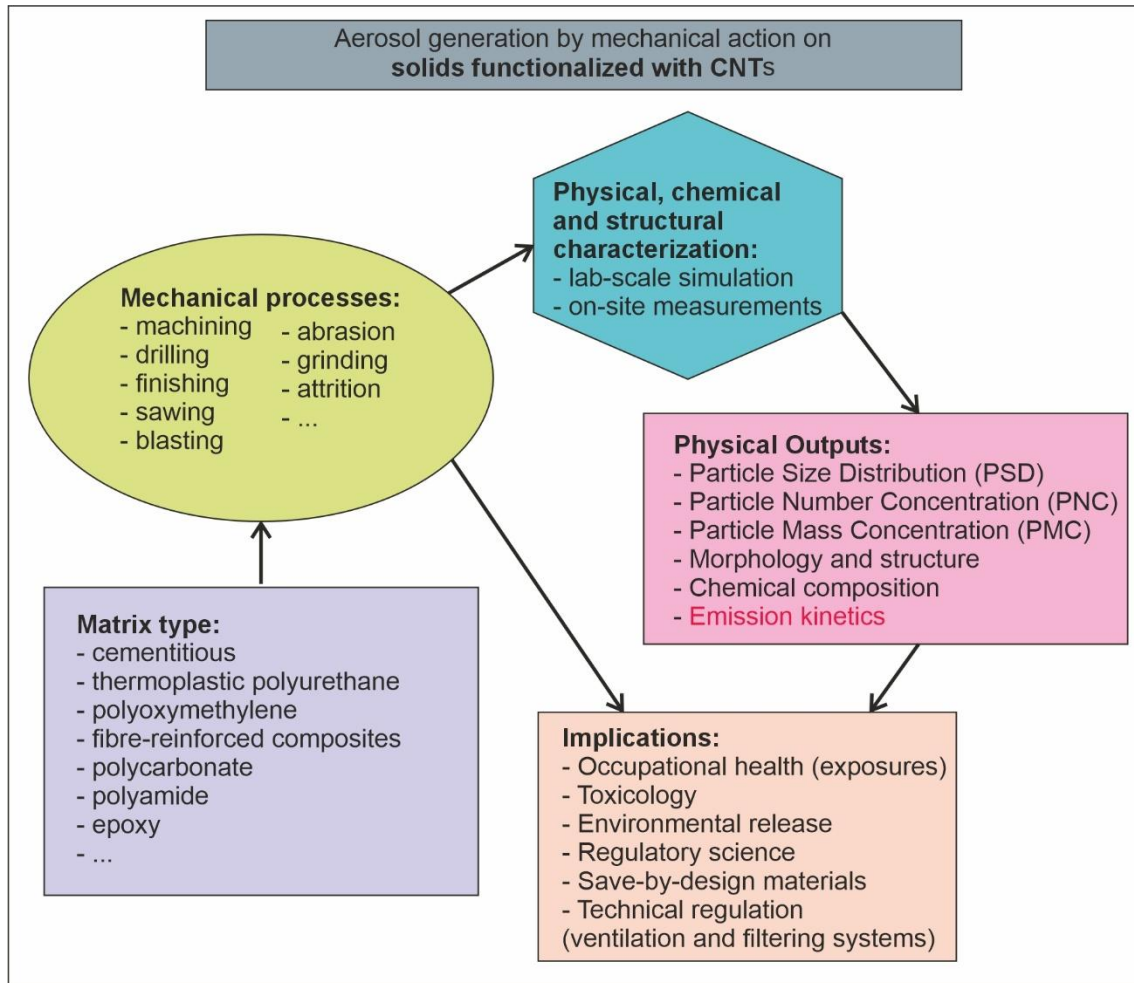


Fig. S3. Schematic of aerosol emission studies from carbon nanotube-containing solids subjected to mechanical action.

6. SEM of the synthesized MWCNTs

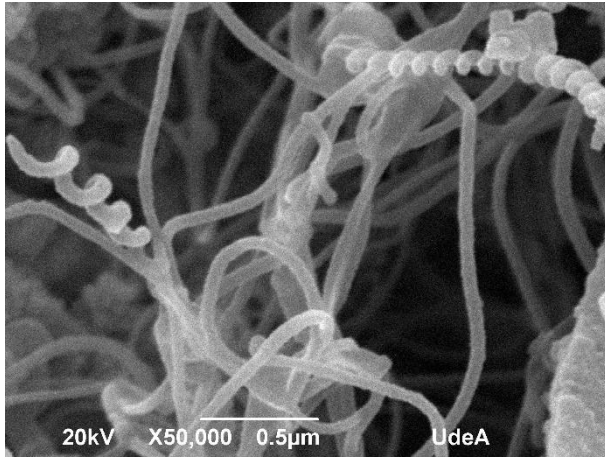


Fig. S4. Scanning electron micrograph of synthesized MWCNTs.

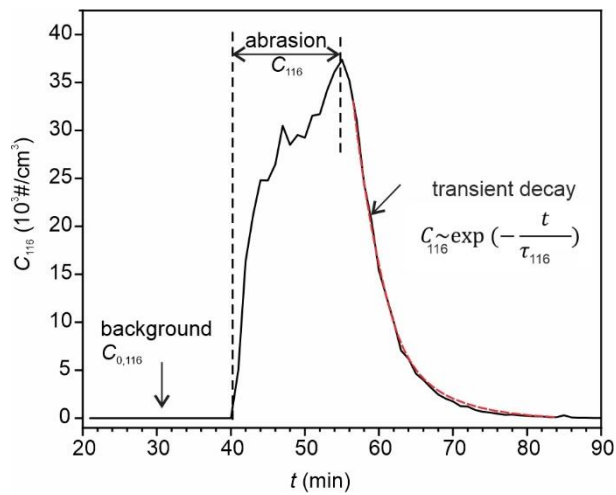


Fig. S5. A representative plot of concentration time series for sample Cem during the triboemission experiment. Particle size range centred at $D_p = 116$ nm. The exponential fit of the experimental data is shown by the red dashed line. $C_{0,116}$ is the background concentration of particles with D_p 116 nm, C_{116} is the concentration of aerosols with D_p 116 nm produced by abrasion, and τ_{116} is the time constant of the transient concentration decay.

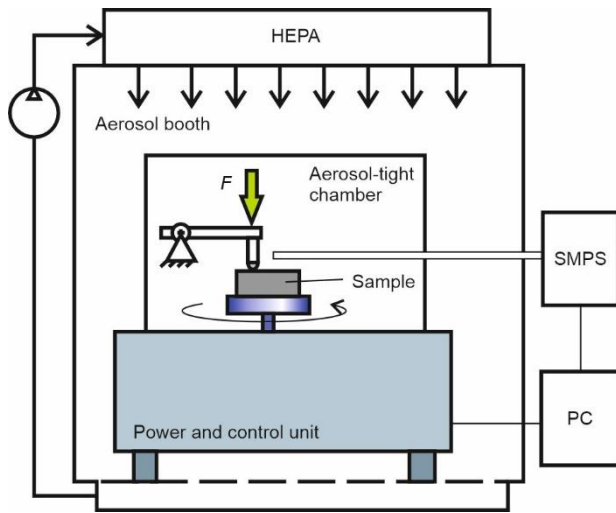


Fig. S6. Schematic drawing of the experimental setup. Adopted from [8] under Creative Common CC BY license.

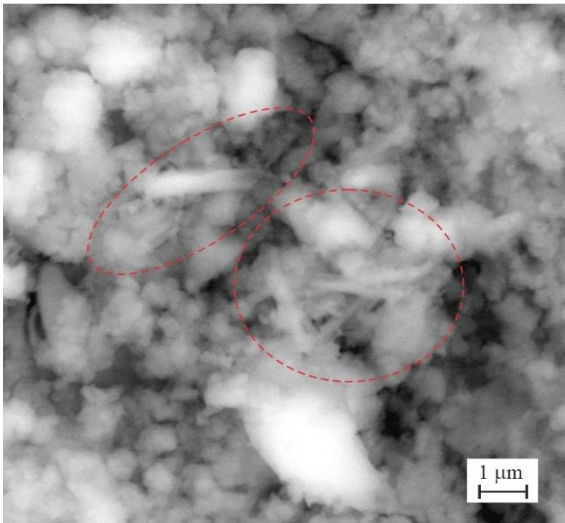


Fig. S7. Magnified micrograph of Cem worn surface showing fibrous or rod-like structures.

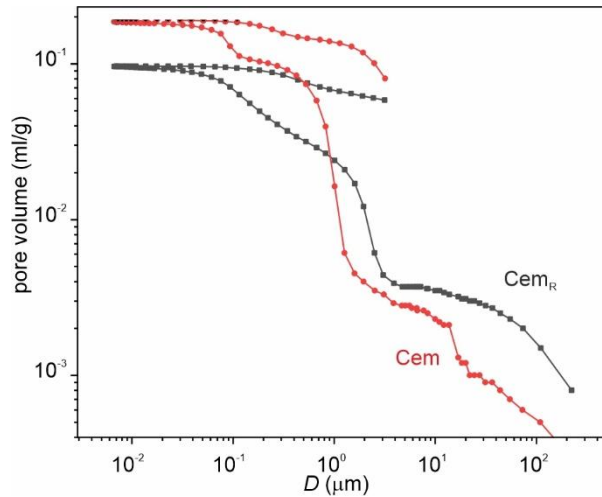


Fig. S8. Distribution of specific pore volume as a function of pore diameter for Cem_R and Cem samples, determined by mercury intrusion.

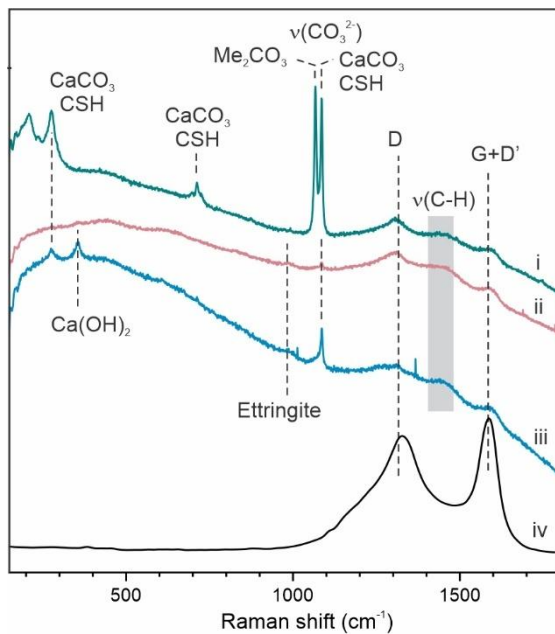


Fig. S9. Raman spectra for i – pristine Cem surface, ii – worn Cem surface, iii – Cem bulk and iv – neat MWCNTs.

References:

- [1] Tian X, Kennedy FE, Jr. Maximum and Average Flash Temperatures in Sliding Contacts. *Journal of Tribology*. 1994;116:167-74.
- [2] Ben Abdelhamid M, Mihoubi D, Sghaier J, Bellagi A. Water Sorption Isotherms and Thermodynamic Characteristics of Hardened Cement Paste and Mortar. *Transport in Porous Media*. 2016;113:283-301.
- [3] Zhou C, Ren F, Zeng Q, Xiao L, Wang W. Pore-size resolved water vapor adsorption kinetics of white cement mortars as viewed from proton NMR relaxation. *Cement and Concrete Research*. 2018;105:31-43.

- [4] Odler I. The BET-specific surface area of hydrated Portland cement and related materials. *Cement and Concrete Research*. 2003;33:2049-56.
- [5] Rouquerol J, Llewellyn P, Rouquerol F. Is the bet equation applicable to microporous adsorbents? In: Llewellyn PL, Rodriguez-Reinoso F, Rouquerol J, Seaton N, editors. *Studies in Surface Science and Catalysis*: Elsevier; 2007. p. 49-56.
- [6] Feng C, Janssen H, Wu C, Feng Y, Meng Q. Validating various measures to accelerate the static gravimetric sorption isotherm determination. *Building and Environment*. 2013;69:64-71.
- [7] Thomas J, Jennings H, Allen A. The Surface Area of Hardened Cement Paste as Measured by Various Techniques. *Concr Sci Eng*. 1999;1.
- [8] Nevshupa R, Castellote M, Cornelio J a C, Toro A (2020). Triboemission of Fine and Ultrafine Aerosol Particles: A New Approach for Measurement and Accurate Quantification. *Lubricants*, 8(2): 21